On relaxing constraints on multi-branch RF front-end for a SIMO OFDM receiver – A global system evaluation scheme

Pierre-Francois Morlat, Guillaume Villemaud, Jacques Verdier, Jean-Marie Gorce

EUROPEAN COOPERATION

IN THE FIELD OF SCIENTIFIC

AND TECHNICAL RESEARCH

———————————————

EURO-COST

———————————————

COST 2100 TD(08) 659

Lille, France

2008/Oct/06-08

SOURCE: CITI, Centre d'Innovarion en Telecom et Intégration de services,
           INSA Lyon,
           France

On Relaxing constraints on Multi-branches RF Front-End for a SIMO OFDM Receiver – A Global System evaluation Scheme

Pierre-François Morlat, Guillaume Villemaud,
Jacques Verdier, Jean-Marie Gorce
CITI/INRIA
21, avenue Jean Capelle
69621 Villeurbanne
France
Phone: + 39-051 20 93 817
Fax: + 39-051 20 93 540
Email: pierre-francois.morlat@insa-lyon.fr

1- Introduction

In today wireless system, the principle of combining OFDM (Orthogonal Frequency Division Multiplexing) scheme and multi-antenna processing (MIMO or SIMO architectures) is often use and offer an important increase of achievable performances. Another objective is to propose more and more integrated systems, and to reduce the space and the cost of the wireless designs. In this way, homodyne down conversion structure appears to be very seductive. Unfortunately, multi-antenna systems and complexity reducing are really contradictive: increasing the number of multi-branches leads to RF components duplication and increase in space occupation. In order to decrease systems cost, the dirty RF concept [1] which aims at identifying constraints that can be relaxed on hardware component is an interesting solution. However, OFDM technique is really sensitive on RF impairments [2] and numerical processing have to be used in order to estimate and correct non-idelallities of the hardware stage to minimize the decreasing of performances transmission due to dirty RF. Especially in the case of the use of an homodyne structure, when RF impairments are much more critical, as compared with super-heterodyne receivers [3]. Three most critical RF impairments have been studied in the special case of OFDM receiver: phase noise [4, 5] and frequency offset [6,7] due to local oscillator non idealities and IQ imbalance due to mismatch between the both I and Q branches especially critical in an homodyne structure [9, 10]. For each considered impairments numerical processing ensuring an impairments defaults exist, but error can still occure and the use of these algorithm increase the numerical complexity of the developed receiver. In this context, the aim of this work is to point out the potential of naturally compensating the RF impairment presented before jointly with the fading effects by the usage of a classical SIMO antenna processing algorithm, thus without increasing numerical complexity in the special context of the often used 802.11g WLAN OFDM transmission [12]. In this current article, main of the presented results are obtained by taking into account most as possible realistic working condition by the use of a global system evaluation scheme based on Agilent Technologies equipments [13]. As presented in [13], realistic consideration of the characteristics of transmission channel, the antenna coupling and also the channel correlation would indeed allow a fast and effective design of multi-antenna wireless systems in order to obtain an important design cycle reducing.

The first part presents the used global system level approach and the associated tools with some theoretical, simulated and measured results in order to validate the developed testbed radio plateform. In the second part, the three presented RF impairments are considered one by one in a Zero-IF down conversion structure and their effect on OFDM transmission performances are detailed. In the last part, after a short description of the SIMO processing that is used, the natural compensation of each RF impairment it is possible to obtained taking advantage of space diversity

is presented. Results given in this part are obtained by taking into account different measured propagation channels (AWGN or fading channels) and a complete 802.11g structure.

2- Description and validation of the global simulation scheme

This part of the work presents the global simulation scheme developed in order to efficiently simulate and measure all part of a SIMO (Single Input Multiple Output) 802.11g transmission chain from the global system level down to the particular model of RF components or fading channels. [13] presents the testbed radio platform developed using Agilent Technologies equipments: the ADS software and the measurement hardware (two arbitrary waveform generators - ESG 4438C - and a vector spectrum analyzer with two RF inputs - VSA 89641). Due to the capabilities of the developed platform, realistic 2x2 MIMO transmissions, extending measurements up to 6 GHz, with a received bandwidth analysis of 36 MHz could be experimented (Fig. 1).
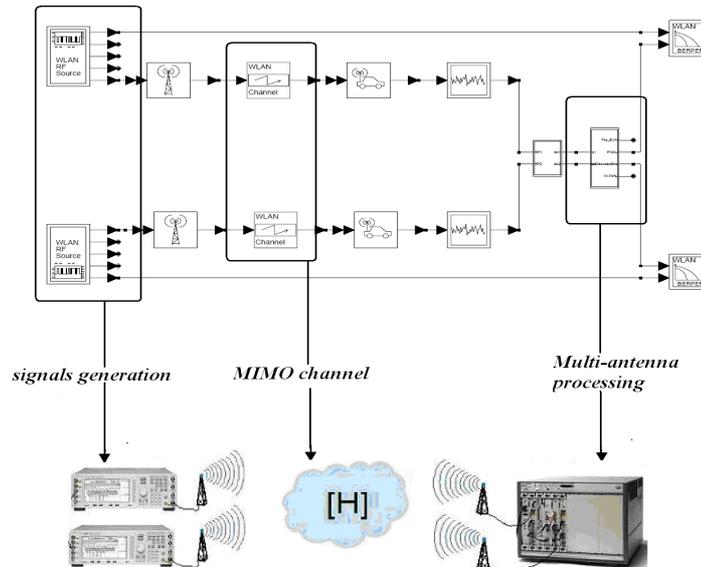
Figure 1 - The 2x2 MIMO connected solution using the interaction between ADS software and Agilent Technologies equipments. Emitter part, channel propagation and receiver part can be studied and modelled.

In order to validate the developed testbed platform, the first tests were done for an uncoded 36 Mbps 802.11g SISO transmission, under an AWGN propagation channel simulating a perfect Zero-IF base band conversion stage. For such a data rate, a 16-QAM modulation scheme is used. The theoretical Symbol Error Probability P_s for a M-QAM is computed considering two independent $\sqrt{M}$ PAM modulations on both I-and Q-channels:

$$P_s = 1 - \left(1 - P_{\sqrt{M}}\right)^2 \tag{1}$$

with :

$$P_{\sqrt{M}} = 2\left(1 - \frac{1}{\sqrt{M}}\right)Q\left(\sqrt{\frac{3\log_2(M)}{M-1}\gamma_b}\right) \tag{2}$$

where γ_b denotes the energy per bit to noise ratio (Eb/No) and Q the Gaussian function. The relationship between the Signal to Noise Ratio (SNR), the transmission data rate, the coding rate R_c, the signal bandwidth (BW) and γ_b is given by:

$$SNR = \frac{data\_rate \cdot R_c}{BW} \cdot \gamma_b \tag{3}$$

Where BW = 20 MHz, and R_c =3/4 in the case of a 802.11g transmission.

In the end, the theoretical Bit Error Probability (BER) is:

$$BER = \frac{P_s}{\log_2(M)} \tag{4}$$

Fig. 2 compares simulated, measured and theoretical BER for an uncoded 36 Mbps 802.11g (16-QAM) transmission. In order to obtain a targeted BER value estimation (variance of 10^{-2}), 10 000 frames of 200 bytes are transmitted in measure and simulation tests for each SNR value. AWGN measures were not made in anechoid chamber but in close and static line of sight working conditions. A good matching between the different data can be observed (deviation is around only 1 dB). Unless stated otherwise, all described results were obtained with real simulated 802.11g structure using 52 OFDM data sub-carriers, convolutionnal error correcting code, Viterbi decoder and soft decision technique. The transmission data rate is 36 Mbps.
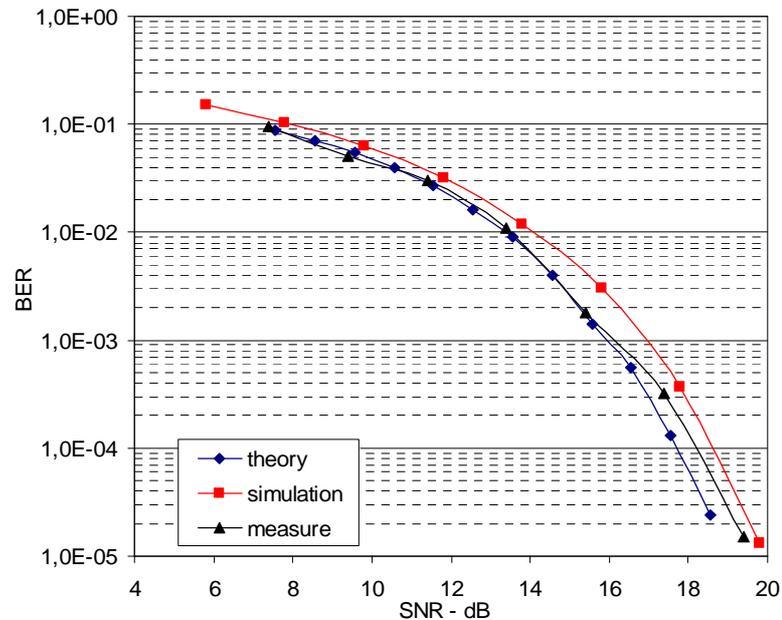
Figure 2 - Uncoded 802.11g AWGN BER performances. Theoretical, simulated and measured data are plotted versus SNR.

3- RF impairment SISO effects

3.1 Notations

Three RF impairments at the receiver side are taken into account. Our work focuses on the effect of frequency offset, the local oscillator (LO) phase noise, the I-Q imbalance (both gain and phase). Fig. 3 presents the structure of a Zero-IF converter including the RF impairments considered in our study. To ease readability, the low pass filter stage and the ADC are intentionally omitted even though they are also responsible for I-Q imbalance.

θ (rad) and α (V) refer to phase and gain imbalance respectively; Δf (Hz) is the mismatch between the carrier frequency f_c of the emitter and the receiver; φ is the phase noise due to local oscillator imperfection. The gain imbalance G is given in dB by:

$$G = 20 \log\left(\frac{1+\alpha}{1-\alpha}\right) \tag{5}$$

The frequency offset value is often expressed in parts per million:

$$\Delta f_{ppm} = \frac{\Delta f(Hz)}{f_c} \tag{6}$$
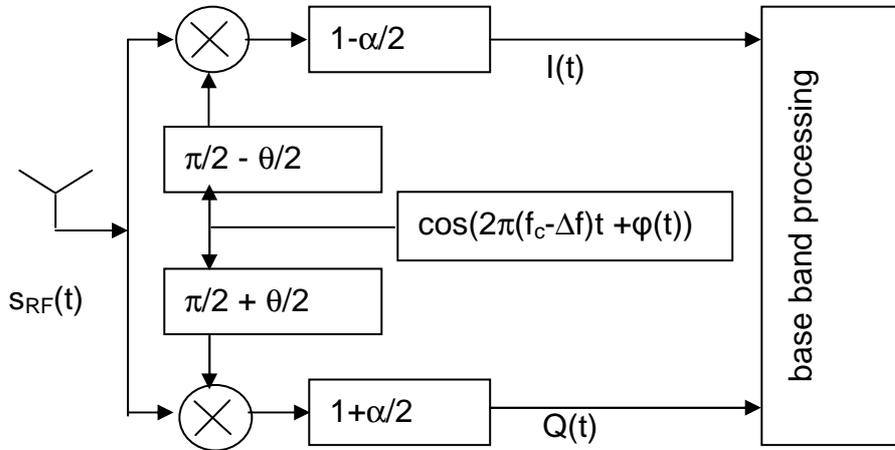
Figure 3 – Zero-IF converter with RF impairments (local oscillator phase noise, frequency offset and I-Q imbalance).

x(t), *y(t)* and *z(t)* (to be introduced later) denote the complex emitted signal, the received signal after channel propagation without RF impairments, and the baseband signal after RF impairment degradation in the temporal domain, respectively. *h(t)* and *n(t)* refer to the temporal channel impulse response and the additive white Gaussian noise, respectively. The same notation using capital letters refers to the transposed signals in the frequency domain. $\otimes$ is the convolution operator, and *

denotes complex conjugation. M is the number of sub-carrier used in the OFDM system (M=64 for a 802.11g transmission).

Most of the presented performances are given in relative BER (i.e. ratio between BER with imperfection and BER with perfect RF conditions). Reference BER is about 5.10^{-3}. This is obtained for a perfect simulated Zero-IF down converter. To have a precise estimation of relative BER, 3000 measurements or simulated frames of 1600 bit are performed.

3.2 Phase noise effect

Phase noise effect can be separated into a multiplicative and an additive part in single-input single output OFDM systems. Due to phase noise impairments φ(t), the temporal received signal is defined by

$$z(t) = [h(t) \otimes x(t)] \cdot e^{j\varphi(t)} + n(t) \tag{7}$$

After removing the cyclic prefix and applying the DFT on the remaining samples, the demodulated carrier amplitudes $Z_m(k)$ with k the sub-carrier index ($0 < k < M - 1$) of the mth OFDM symbol are given by [14]

$$Z_m(k) = H_m(k)X_m(k)\underbrace{S_{m,0}}_{CPE} + \underbrace{\sum_{l=0,l \neq k}^{M-1} X(l)H(l)S_{m,l-k}}_{ICI} + N_m(k) \tag{8}$$

The term $S_{m,i}$ corresponds to DFT of one realization of $e^{j\varphi(n)}$ during the mth OFDM symbol:

$$S_{m,i} = \frac{1}{M}\sum_{n=0}^{M-1} e^{-j(2\pi n i/M + \varphi(n))} \tag{9}$$

The received sample in frequency domain (8) exhibits two terms due to phase noise. All phase noise correction schemes are based on Common Phase Error (CPE) estimation and mitigation, and are relatively efficient in WLAN OFDM systems for small phase noise working conditions. However, under high phase noise, the Inter-Carrier Interference (ICI) term dominates over the CPE. In this case, the phase noise suppression becomes really difficult [6] and the performances requirement may not be guaranteed due to the loss of orthogonality between sub-carriers.

The most common way of characterizing oscillator's phase noise is its Power Spectral Density (PSD), $S_\varphi(f)$, where f is the frequency offset to the carrier frequency. The phase noise effect is commonly characterized as a Wiener process corresponding to a PSD slope of -20dB/dec. In this case, the critical parameter of the oscillator quality is the single sideband -3 dB bandwidth of the Lorentzian power density β. The phase noise variance is hence computed as $\sigma_\varphi^2 = 4\pi\beta T$, with T being the sample time [6]. [4] gives the variance expression for a model more general than the

classical Wiener process, closer to the measurements and which studies the influence of different phase noise spectrum slopes on the system performance:

$$\sigma_\varphi^2 = \int_{-\infty}^{\infty} S_\varphi(f)df \tag{10}$$

When no phase noise suppression algorithm is applied, [4] shows that the Energy per Symbol Ratio degradation D (in dB) caused by phase noise defined by any PSD spectrum - assuming phase noise variance is small ($\sigma^2 \ll 1$) - is not dependent on the number of sub-carriers, and is given by:

$$D = 10\log\left(1 + \sigma^2 \gamma_s\right) \tag{11}$$

γ_s denotes the initial Energy per Symbol Ratio without phase noise impairments.

Fig. 4 shows a comparison between simulated and theoretical BER performance for an uncoded 16-QAM OFDM 802.11g transmission in AWGN propagation condition. These results were obtained considering a phase noise with a PSD spectrum for positive frequencies modelled as follows, and which correspond to a phase noise variance of $\sigma^2 = 0.015$ rad^2 :

-60 dBc/Hz	at 1 kHz
-90 dBc/Hz	at 100 kHz
-110 dBc/Hz	at > 1 MHz
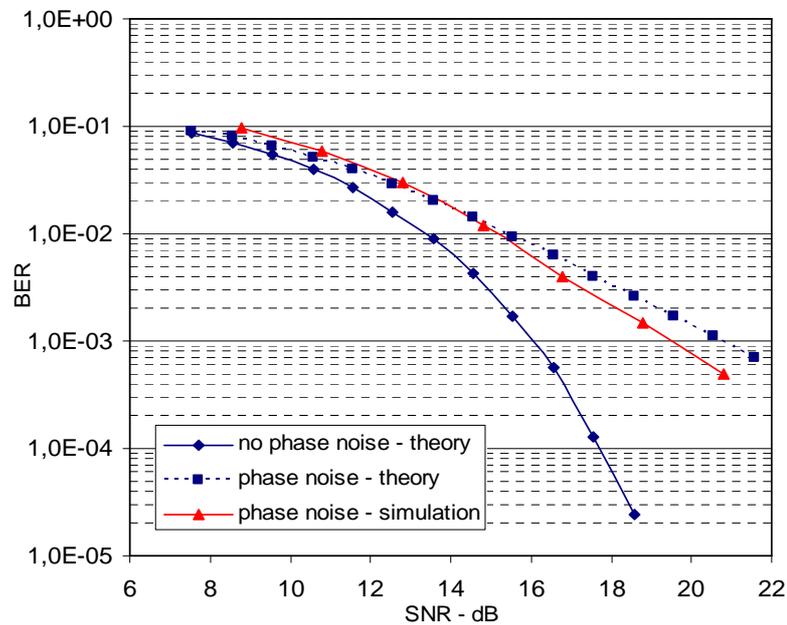
Figure 4 – Phase noise impact on AWGN SISO BER performances (theoretical and simulated data). Phase noise value of local oscillator: [1 kHz @ -60 dBc/Hz, 100 kHz @ -90 dBc/Hz, 1 MHz @ -110 dBc/Hz].

We observe relatively good matching between the results obtained with the developed ADS 802.11g transmission scheme and the analytical results. However, it is important to note that in many WLAN OFDM receivers, CPE correction is applied (see [20] for example). As CPE can

easily be suppressed, only ICI distribution has to be considered to compute SNR penalty. The properties of the ICI term were previously studied by several authors. In many cases, only a Wiener process is considered and the ICI term is assumed to be complex Gaussian distributed. This approximation is valid only for small phase noise process [14]. As explained in [5], it is important to take into account different slopes values in the phase noise spectrum to provide applicable models for hardware design. Our developed test-bed answers this need, but it is not the aim of this work.

3.3 Frequency offset

The complex baseband received signal affected by frequency carrier mismatch between the receiver and the emitter's local oscillator is:

$$z(t) = [h(t) \otimes x(t)] \cdot e^{-j2\pi\Delta_f t} + n(t) \tag{12}$$

We define the normalized frequency offset ε as the ratio between the carrier frequency offset in Hz and the adjacent OFDM sub-carrier spacing. In the expression below, BW is the occupied signal bandwidth (recalling that BW = 20 MHz for 802.11g transmissions):

$$\varepsilon = \frac{\Delta_f \cdot M}{BW} \tag{13}$$

[8] gives the expression of the sampled signal for the sub-carrier k (k=0,…, M-1) after the receiver fast Fourier transform processing:

$$Z(k) = H(k)X(k)\underbrace{S_0}_{CPE} + \underbrace{\sum_{l=0,l\neq k}^{M-1} S_{l-k}H(l)X(l)}_{ICI} + N(k) \tag{14}$$

Where the sequence S_{l-k} is given by:

$$S_{l-k} = \frac{\sin[\pi(l-k+\varepsilon)]}{M \sin\left[\frac{\pi}{M}(l-k+\varepsilon)\right]} e^{\left[j\pi\left(1-\frac{1}{N}\right)(k-l+\varepsilon)\right]} \tag{15}$$

For a quick evaluation, [6] gives a well-known good approximation of the Energy Per Symbol γ_s degradation D (in dB) for an M-QAM OFDM transmission:

$$D = \frac{10}{\ln(10)}\frac{1}{3}(\pi\varepsilon)^2\gamma_s \tag{16}$$

Fig. 5 compares BER performances of an uncoded 16-QAM OFDM transmission under an AWGN propagation channel, taking into account a frequency offset equal to 8.3 ppm (Δ_f = 20 kHz). The fact that the different curves match validates our structures and measurement methods.
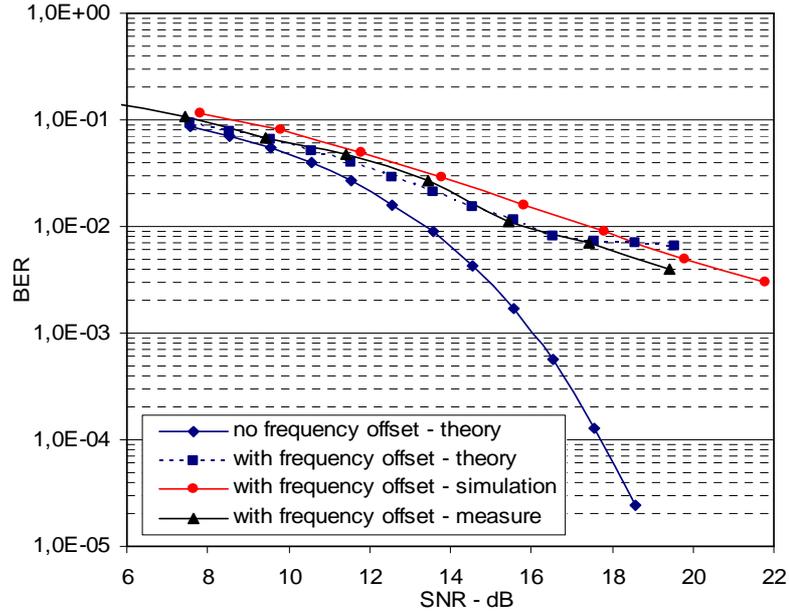
Figure 5 – Frequency offset impact on AWGN SISO BER performances (theoretical, simulated and measured data). The frequency offset value is 20 kHz.

3.4 I-Q imbalance

The imbalance can be modelled either symmetrical or asymmetrical (these are equivalent representations). In the symmetrical method which is used here [11], each arm (I and Q) experiences half of the phase and amplitude errors. It has been shown that multi-carrier signals are affected by a mutual inter-carrier interference between each pair of symmetric sub-carriers [10].

The perfect baseband received signal after channel propagation is given by:

$$y(t) = h(t) \otimes x(t) + n(t) \tag{17}$$

[10] gives the expression of the imperfect baseband signal due to I-Q imbalance

$$z(t) = \mu \cdot y(t) + \lambda \cdot y(t)^* \tag{18}$$

Injecting (18) in (17), one can show that

$$z(t) = \mu \cdot [h(t) \otimes x(t) + n(t)] + \lambda \cdot [h(t) \otimes x(t) + n(t)]^* \tag{19}$$

where μ and λ depend on the I-Q imbalance:

$$\begin{cases} \mu = \cos\left(\dfrac{\theta}{2}\right) + j\alpha\sin\left(\dfrac{\theta}{2}\right) \\[2mm] \lambda = \alpha\cos\left(\dfrac{\theta}{2}\right) - j\sin\left(\dfrac{\theta}{2}\right) \end{cases} \tag{20}$$

In the frequency domain, for each data sub-carrier k of the OFDM signal ($k \in [-26, 26]$), the received signal is given by

$$Z(k) = \mu H(k) X(k) + \lambda H(-k)^* X(-k)^* + \mu N(k) + \lambda N(-k)^* \tag{21}$$

[10] shows that the error Δ between the estimated received symbol and the emitted symbol for each sub-carrier k due to the I-Q imbalance is

$$\Delta(k) = \frac{\lambda}{\mu} \frac{H(-k)^*}{H(k)} X(-k)^* + \frac{1}{H(k)} N(k) + \frac{\lambda}{\mu} \frac{1}{H(k)} N(-k)^* \qquad (22)$$

[15] gives the analytical BER expression for M-QAM OFDM systems in the presence of I-Q imbalance, based on constellation degradation. Fig. 6 presents, in the case of AWGN transmission, uncoded 16 QAM-OFDM BER performances by using the presented radio communication platform.
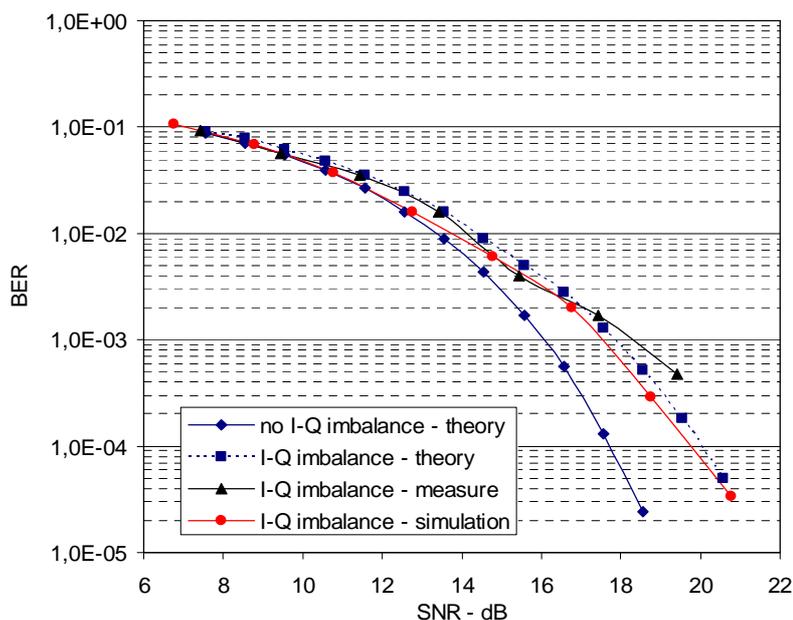
Figure 6– I-Q imbalance impact on AWGN SISO BER performances (theoretical, simulated and measured data). The phase imbalance value is 5° and the gain imbalance is equal to 0.6 dB.

Simulated and measured data are compared with theoretical results. In this figure, phase imbalance and gain imbalance are respectively equal to θ=5° and α=0.6 dB.

4- RF impairments mitigation using SIMO processing

4.1 The SIMO 802.11g architecture

Spatial diversity is very often considered in today radio receiver ensuring BER performances improving by the use of SIMO processing. Instead of using only one antenna at the receiver side, N antennas are used to take advantage of the several versions of the same emitted signal, combining these N signals and increasing the SNR of the received signal.

In our case, a Minimum Mean Square Error (MMSE) approach is used as the optimization criterion using a Sample Matrix Inversion (SMI) technique [16] to estimate the optimal complex weight to

apply on each received branch. These coefficients are computed using the knowledge of the two long preambles (corresponding to two OFDM symbols) at the beginning of each 802.11g frame in the frequency domain. Considering a constant propagation channel response during the complete frame duration, the SMI processing ensures a very good trade-off between BER performance and computation complexity.

In our equipment, the two incident signals are recorded simultaneously by the VSA, and the baseband signals are re-injected in the ADS simulated multi-antenna structure. Simulated and measured performances of 1x2 SIMO structures for different propagation channels and in realistic working conditions are presented in [18]. In the next part of this work, we present the effect on RF impairments due to a non-ideal Zero-IF baseband converter. Even if adapted numerical processings already exist to decrease and correct RF impairments, some errors can still occur. That is why it seems to be an interesting study to detail the natural compensation due to SMI properties it is possible to reach. Furthermore, this kind of study corresponds well on the context of a global system performances presentation.

4.2 Phase Noise Mitigation

As detailed in section 3, local oscillator phase noise impacts M-QAM OFDM transmission significantly. Even if CPE can be removed, residual errors due to ICI still exist. Furthermore, the design of precise local oscillators ensuring a decreasing phase noise variance is expensive. That is why we present, in this part, the achievable performances in a SIMO configuration for different propagation channels including phase noise impairment. The considered phase noise PSD is modelled as follow:

$$-60 \text{ dBc/Hz} \qquad \text{at } \beta \text{ Hz}$$
$$-80 \text{ dBc/Hz} \qquad \text{at } \beta \text{ x10Hz}$$
$$-100 \text{ dBc/Hz} \qquad \text{at } > \beta \text{ x100 Hz}$$

This corresponds to a Wiener phase noise exhibiting a -20dB/dec slope with β the PSD spectrum bandwidth of the phase noise. With β increasing, SNR degrades and hardware components get cheaper.

Fig. 7 gives the relative BER performances obtained by simulation considering a complete 802.11g transmission scheme: both phase tracking ensuring CPE suppression and FEC decoding are applied. AWGN and frequency selective channels with fading are used to simulate the wireless propagation. The parameter β takes different values between 1 kHz and 30 kHz, i.e. between $3.2.10^{-3}$ and $9.6.10^{-2}$ the OFDM sub-carrier spacing of 312.5 kHz.

As showed in Fig. 9, SIMO processing does not mitigate phase noise impairments significantly, especially under the AWGN case. This result can be explained by the fact that the optimal complex

coefficients applied on each arm of the SIMO receiver are estimated with only the 128 samples of the 802.11g frame preamble (2 OFDM symbols). However, as reported in (8) and (9) the phase noise contribution is not constant during a whole frame, and takes different values at each new OFDM symbol; the SIMO weights become obsolete. This observation could be mitigated if the transmission is under a frequency selective channel. In this case, the multi-antenna receiver is able to take advantage of spatial diversity and $H(k)S_{k-l}$ can take small values on each received branch, ensuring a decreasing of the ICI term.
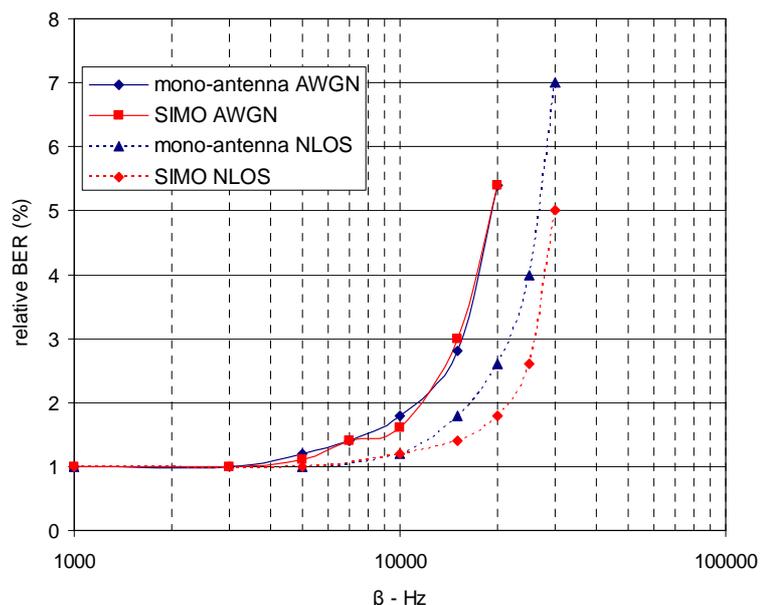
Figure 7 – Phase noise mitigation in AWGN and NLOS simulated conditions. Results are given in relative BER versus local oscillator phase noise characteristics (β)
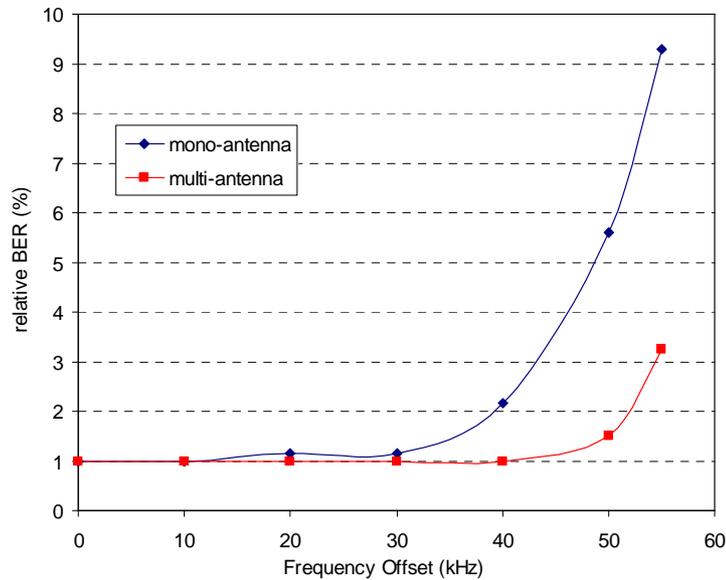
4.3 Frequency Offset Mitigation

In a common 802.11g receiver, digital stages of frequency offset estimation and correction are implemented [19]. However, residual frequency offset can occur, and introduce errors in the propagation channel estimation. SIMO performance evaluation in a realistic 802.11g structure seems to be an interesting choice and is detailed in the next part.

Fig. 8 presents the BER relative performances for different frequency offset values, in the range of 0 to 55 kHz (i.e. 0 to 23 ppm). These results were obtained by treating measured signal in the case of an NLOS with fading transmission. Even though the frequency carrier offset takes an important value of 50 kHz, the impact of this impairment that is obvious for a SISO transmission is really well mitigated using diversity.

Even if the analytical impact of frequency offset and phase noise on the received complex samples are almost the same, we observe that SIMO processing ensures larger mitigation of frequency offset

than of phase noise impairment. This is due to the fact that the ICI term is constant in the case of a transmission impaired by frequency offset. Hence, this constant error is taken into account by the SIMO processing and complex weights computed by MMSE algorithm are still optimal during the entire frame (from a frequency offset mitigation point of view).


Figure 8 – Relative BER versus frequency offset in NLOS working conditions. SISO and 1x2 SIMO performances are given.

4.4 I-Q mismatch mitigation

At first, SMI gain related to simultaneous measured signals is presented in Fig. 9 for an I-Q phase imbalance in the range of 0° to 10°. The solid line curves represent BER performance for an AWGN propagation channel. This clearly shows that the SMI algorithm efficiently compensates RF impairments impact, even for a large phase imbalance of 10°, and that SIMO processing allows a very good rejection of the jamming effect due to phase imbalance. In the case of a wireless link under a frequency selective and fading channel, performance degradation and their mitigation with the SMI processing are presented with dotted lines on the same figure. SISO performances under AWGN and NLOS working conditions are fairly close, which seems contradict (22). A possible explanation is related to the noise level at the receiver input. In the present case, the reference BER value of 5.10^{-3} is relative high, so the contribution of the first term in (22) is not significant. Furthermore, the I-Q impairments mitigation with the SMI processing is less important for frequency selective working conditions than for a transmission under an AWGN channel. This could be explained by (22) when reminding that the same complex weights are applied to all the

sub-carriers. The mitigation difference clearly appears for phase imbalance of up to 8°, which is an important mismatch.
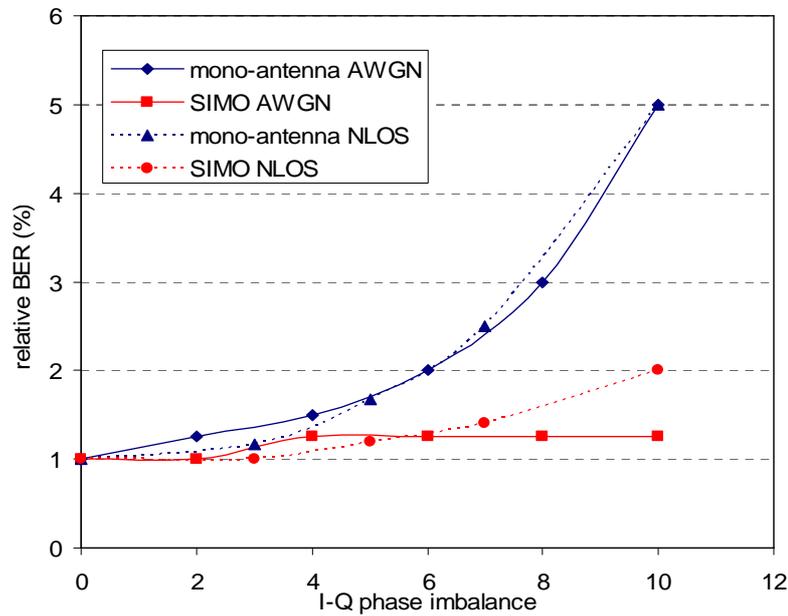
Figure 9 - Relative BER versus I-Q phase imbalance in AWGN and NLOS measured working conditions. SISO and 1x2 SIMO performances are given.
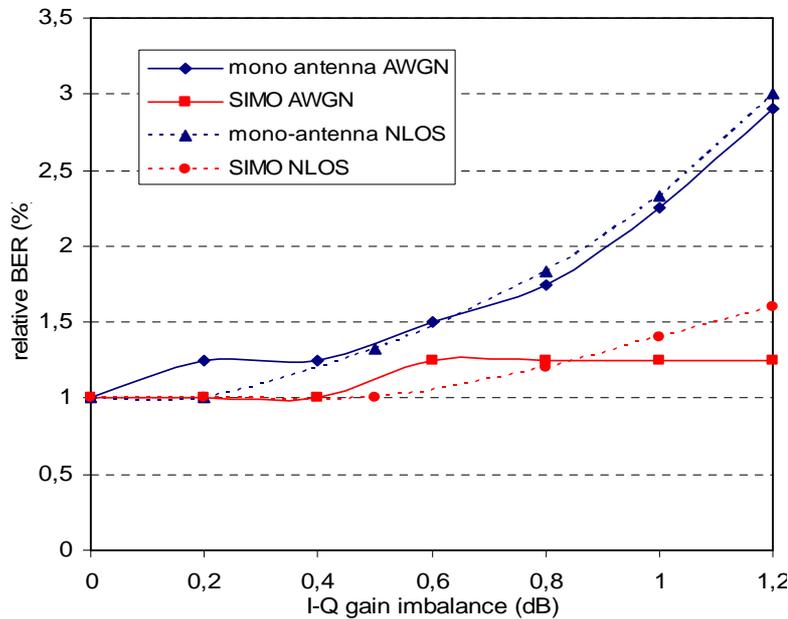
Figure 10 – Relative BER versus I-Q gain imbalance in AWGN and NLOS measured working conditions. SISO and 1x2 SIMO performances are given.

Following the same approach, I-Q gain imbalance influence was studied. Fig. 10 presents the mitigation which can be reached using diversity for different I-Q gain imbalance values from 0 to 1.2 dB. Similar conclusions can be drawn for I-Q gain imbalance mitigation with SMI processing.

Even if the mitigation with the SMI algorithm is less important in multi-path propagation channels than in AWGN conditions, excellent performance can be observed for I-Q gain imbalance values up to 1 dB.

5- Conclusion

We present a comprehensive study of a multi-antenna OFDM homodyne receiver, based on theory, simulation and measurements with a reduced design cycle results. The aim of this approach is to get a realistic view of a complex system's performance without requiring many stages of prototyping. This study highlights the key points of the RF element design for this kind of receiver.

The multi-antenna approaches, as software radio principles, call to reduce strains on the quality of components to achieve an acceptable cost-performance ratio. We prove that the conventional multi-antenna treatment used can significantly reduce damage caused by the most common RF impairments: frequency offset, local oscillator phase noise and IQ imbalance. The multiplication of RF branches can be made cheaply if we consider this natural impairments compensation, without ever having to resort to specific digital processing. The result, however, is that particular attention should be paid to the problems of phase noise, by the means of a strong constraint on the selected components, or by the addition of a dedicated digital processing.

As future work, we plan to assess the same constraints and possible compensations as part of a multi-standard broadband architecture, making it possible to obtain a feasible receiver for applications such as cognitive or opportunistic radio. More results concerning this work are presented in [20].

6- References

[1] G. Fettweis, M. Lohning, D. Petrovic, M. Windish, P. Zillman, W. Rave, "Dirty RF, a new Paradigm", *International Journal of Wireless Information Networks,* Springer, Vol. 14, No. 2, 2007

[2] S. Woo et al, "Combined Effects of RF impairments in the Future IEEE 802.11n WLAN Systems", *IEEE Vehicular Technology Conference Spring 2005*, Vol.2, May 2005

[3] M. Brandolini, P. Rossi, D. Manstrett and F. Svelto, "Toward Multi-Standard Mobile Terminals – Fully Integrate Receivers Requirements and Architecture", *IEEE Transaction On Microwaves Theory and Techniques*, vol. 53, No 3, 2005.

[4] A.G. Amrmanda, "Understanding the effects of Phase Noise in Orthogonal Frequency Division Multiplexing (OFDM)", *In Proc. of IEEE Transactions on Broadcasting*, Vol. 47, No. 2, 2001.

[5] R. Corvaja, S. Pupolin, "Phase Noise Spectral Limits in OFDM Systems", *Wireless Personal Communications*, Springer 2006.

[6] T. Pollet, M. Van Bladel, M. Monoeclaey, "BER Sensitivity of OFDM Systems to Carrier Frequency Offset and Wiener Phase Noise", *In Proc IEEE Transactions on Communications*, Vol. 43, No 2, pp 191-193 1995.

[7] X.Ma, H. Kobayashi, S.C. Schwartz, "Effect of frequency offset on BER of OFDM and Single Carrier Systems", *Proceedings of 14th IEEE International Symposium on Personal, Indoor and Mobile Radio Communication*, 2003.

[8] J. Armstrong , "Analysis of new and existing methods of reducing intercarrier interference due to carrier frequency offset in OFDM", *IEEE Transaction on Communications*, vol. 47, pp 365-369, 1999.

[9] M. Windish, G. Fettweis, "Performance Degradation due to IQ imbalance in Multi-Carrier Direct Conversion Receivers: A Theoretical Analysis", *IEEE International Conference on Communications*, ICC, 2006.

[10] C.L. Liu, "Impact of IQ imbalance on QPSK OFDM QAM detection, *IEEE Transactions on Consumers Electronics,* vol. 44, No. 3, pp984-989, 1998.

[11] J. Tubbax, B. Come, L. van der Perre, L. Deneire, S. Donnay, M. Engels, "Compensation of IQ imbalance in OFDM systems", *in Proceedings of IEEE International Conference on Communications*, 2004, pp 3403-3407.

[12] IEEE Std 802.11g-2003, Part 11: Wireless LAN Medium Access Control (MAC) and Physical Layer (PHY) specifications: Further Higher Data Rate Extension in the 2.4 GHz Band.

[13] http://eesof.tm.agilent.com/products/ads_main.html.

[13] P-F. Morlat, H. Parvery, G. Villemaud, J. Verdier, J-M. Gorce, "A Global System Evaluation Scheme for Multiple Antennas Adaptive Receiver", *Proceedings of IEEE European Conference on Wireless Technologies*, Manchester, UK, 2006.

[14] D. Petrovic, W. Rave, G. Fettweis, "Properties of the Intercarrier Interference due to phase noise in OFDM", *In Proc. of International Conference on Communications (ICC)*, Vol.4, 2005.

[15] H. Zareian, V.T. Vakili, "Analytical BER Performance of M-QAM-OFDM Systems in the Presence of IQ imbalance", *in Proceedings of IEEE Wireless and Optical Communications Networks Conference*, Singapore, 2007.

[16] I. J. Gupta, "SMI adaptive antenna arrays for weak interfering signals", *IEEE Transactions on Antennas and Propagation*, vol. AP-34, no. 10, pp 1237-1242, Oct. 1986.

[18] P-F. Morlat, X. Gallon, G. Villemaud, J.M. Gorce "Measured Performances of a Multi-standard SIMO receiver", *EUropeean Conference on Antennas and Propagation*, EuCAP 07, Edinburgh.

[19] V.P. Gil Jimenez, M.J. Fernandez Garcia, F.J Gonzales Serrano, A. Garcia Armanda, "Design and Implementation of Synchronization and AGC for OFDM-based WLAN Receivers", *IEEE Transaction on Consumer Electronic*, Vol. 50, No 4, Nov 04.

[20] P.-F. Morlat, G. Villemaud, J. Verdier, J.-M. Gorce, "On Relaxing constraints on Multi-branches RF Front-End for a SIMO OFDM – A Global System Evaluation Scheme", *IEEE Transaction on Wireless Communication (Submitted to).*